HTML ABSTRACT + LINKS

Phenomenological theory of tunnel emitter transit time oscillators for the terahertz range

Z. S. Gribnikov[a)]
Institute for Quantum Sciences, Michigan State University, East Lansing, Michigan 48824 and Department of EECS, University of Michigan, Ann Arbor, Michigan 48109

N. Z. Vagidov
Department of EE, State University of New York, Buffalo, New York 14260

G. I. Haddad
Department of EECS, University of Michigan, Ann Arbor, Michigan 48109

(Received 15 September 2003; accepted 30 October 2003)

We develop an analytic theory based on an earlier model of the admittance of a ballistic transit time diode terahertz oscillator with tunnel emission of electrons into a transit space. The focus of this work is on the actual case when electrons are injected with high enough energy to move from the start with maximal (saturated) ballistic velocity ($\sim 1\times 10^8$ to 2×10^8 cm/s). On the one hand, such diodes have maximal oscillation frequencies and, on the other hand, a simple analytic theory describes them and allows us to avoid a cumbersome numerical procedure, which characterizes the general case. Such a description is analogous to the description of oscillatory diodes with diffusive transport and saturated drift velocity. We have also considered a special case when a small part of the ballistic electrons crossing the transit space scatter into a diffusive subsystem with a small drift velocity. The appearance of such slow-drifting electrons substantially increases space charge in the transit space and influences the static JV-characteristic but the high-frequency admittance is almost invariable. © *2004 American Institute of Physics.* [DOI: 10.1063/1.1635645]

I. INTRODUCTION

Transit time diodes with a tunnel electron emitter (TUNNETT-diodes,[1–5] hereafter referred to as T diodes) suggested by Nishizawa and Watanabe[1] and later by Aladinski[2] are in principle the highest-speed transit time diodes and are appropriate for the terahertz (THz) range oscillatory regime. Contrary to their IMPATT- and BARITT-competitors,[3] T diodes can be completely ballistic devices since the principle of action inherent in them does not require any dissipative processes both in a tunnel barrier and in a transit space (T space). But in practice, this potential speed has not been realized up to now because as usual the traditional $p^{++}n^{+}nn^{+}$-design[4–6] is used with a tunnel electron emitter in the form of the $p^{++}n^{+}$-junction, which is reverse-biased into the regime of the so-called Zener breakdown or, in other words, a tunnel emission through a band gap. To obtain a sufficient tunnel current in this way, one needs a very strong electric field, which in turn requires a voltage drop of $\sim$7–9 V mainly across the n-region. The latter serves as a T space. This means that electron transport in this space is substantially dissipative, and almost all of the electrons are in noncentral L- and X-valleys (in the case of GaAs, InP, InGaAs, and other similar materials for the n-region). A drift velocity for such a transport does not exceed $\sim 10^7$ cm/s, which leads to oscillatory frequency limitation even in the case of very short T spaces. (Note that the authors of Ref. 7 tried to avoid partially the above-described traditional scheme).

In Refs. 8 and 9, a certain scheme for the T diode was suggested and substantiated theoretically. The main elements of this scheme are the following:

(1) The T-diode is a unipolar heterostructural device with only electrons as the current carriers.

(2) The undoped T space is placed between the heavily doped n^+-cathode and n^+-anode, and the n^+-cathode is separated from the T space by the tunnel permeable (transparent) barrier B, which serves as an electron emitter. Such a barrier on the anode side is absent, so our diode is asymmetrical (Fig. 1).

(3) The T space length l is small $[l \leqslant (0.5-0.6) \times 10^{-5}\ \mathrm{cm}]$ in order to provide ballistic or quasiballistic electron transport across the T space. A comparatively small voltage U_l across the T space in the working regime (typical values are $\sim$0.5–0.6 V) pursues the same goal. The small values of this voltage are determined by the positions of noncentral L- and X-valleys in the conduction band. (It is necessary that the electrons emitted into the Γ-valley by the tunnel emitter stay in the same Γ-valley while traveling across the T-space. They should obtain a possibility of scattering to the lowest noncentral valley only at the output into the n^+-anode). A short length of the T-space in combination with moderate voltage across the T-space provides approximate ballisticity of an electron transport with the velocity $\sim V \cong V_S \sim (1-2)\times 10^8$ cm/s (or even higher). The velocity V_S is a maximal (saturated) velocity of Γ-electrons, which have an isotropic nonparabolic dispersion relation

$$\varepsilon(p) = V_S\left(\sqrt{p_S^2 + p^2} - p_S\right), \qquad (1)$$

[a)]Electronic mail: gribnikov@pa.msu.edu

 © 2004 American Institute of Physics

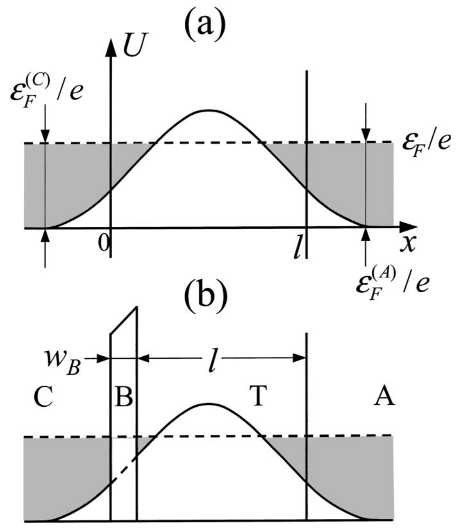

FIG. 1. Equilibrium distribution of an electric potential $U(x)$ in a n^+in^+-structure. (a) Structure without a tunnel barrier. (b) Structure with a tunnel barrier.

where $p_S = mV_S$, and m is an effective mass in the bottom of the Γ-valley.

(4) The boundary T-space/n^+-anode should not reflect electrons coming from the T-space and should also not scatter them back from the n^+-anode. The first condition could be met if the same material were for both the T-space and the n^+-anode. The distinction is only in the doping level: the T-space is undoped, and the n^+-anode is heavily doped. Due to the use of the same material, we have no conduction band discontinuities, which could induce an electron reflection. Because of the above-mentioned substantial distinction in doping level, the bottoms of all the valleys in the n^+-anode lie lower than the same bottoms in the T-space at the boundary T-space/n^+-anode. The difference is approximately equal to the Fermi energy in the n^+-anode, $\varepsilon_F^{(A)}$. (Note, this estimate relates to the working regime: for example, see curve 3 in Fig. 2 and also Fig. 3). Therefore, electrons, which have obtained a kinetic energy near ε_L (where ε_L is a position of a bottom of one of the noncentral valleys) as a result of their ballistic travel in an accelerating electric field across the T-space, have the energy $\sim\varepsilon_L+\varepsilon_F^{(A)}$ after their transfer to the n^+-anode and can scatter into this noncentral valley. As a result of such intervalley scattering, the probability of their return to the T-space decreases noticeably.

In this article, we continue to consider the T diode suggested in Refs. 8 and 9 and use the same phenomenological scheme of description. This scheme is based on the fact that the electrons emitted by the tunnel emitter travel across the T-space in the form of a monoenergetic beam with a near-zero transverse momentum: $\vec{p}_\perp \cong 0$. Electrons in this beam are accelerated by a longitudinal electric field $E(x)$. The latter is the sum of a large dc field and a small high-frequency monochromatic field (with an angular frequency $\omega = 2\pi f$). The ballistic transport is described by classical mechanics equations. Reducing the transport problem to the consideration of a monoenergetic electron beam (with the collectivized electron velocity, momentum, and energy) is first based on the electron transport ballisticity in the

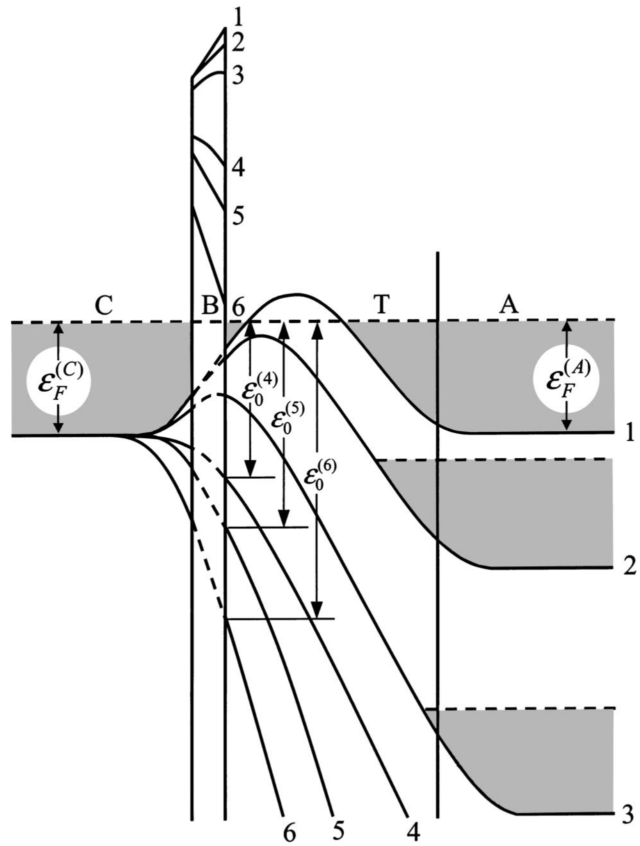

FIG. 2. Qualitative sketch of nonequilibrium potential distributions in the considered T diode structure. Curve 1 corresponds to the equilibrium picture. The curve number increases with an increase in voltage across T diode. Curves 2 and 3 correspond to potential distributions with a virtual (effective) cathode inside T space. For curves 4, 5, and 6, a virtual cathode disappears and a depletion layer in n^+-cathode is replaced by an accumulation layer, which becomes deeper and deeper with an increase in the applied voltage. We can see a lowering of the effective barrier height over the Fermi level in n^+-cathode and an increase in energy ε_0 of electrons entering T space: $\varepsilon_0^{(6)} > \varepsilon_0^{(5)} > \varepsilon_0^{(4)}$.

T-space: electrons do not scatter, and an energy width of the beam is determined by their initial temperature T in the n^+-cathode. This temperature is assumed to be small on the scale of all other energies in the considered problem. In the second place, the tunnel transparency of the tunnel barrier emitter at $\varepsilon = \varepsilon_F^{(C)}$ is also assumed to be sufficiently low and rapidly decreasing with a drop in energy (starting from its level on the Fermi surface). This means that the above-mentioned electron beam in T-space is formed by electrons with energy $\varepsilon = \varepsilon_F^{(C)}$ counted from the bottom of the conduction band in the depth of the n^+-cathode. These electrons have comparatively little transverse momentum: $\vec{p}_\perp \cong 0$. In comparison with Refs. 8 and 9, we have changed the assumed design of the tunnel barrier emitter. It has been selected so that electrons can be injected in the Γ-valley of the T-space with a sufficiently large initial kinetic energy $\varepsilon(x=0) = \varepsilon_0$ and the corresponding initial longitudinal momentum $p_X = p_0$ where $\varepsilon(p_0) = \varepsilon_0$. Since we have assumed in the Γ-valley the isotropic nonparabolic dispersion relation [see Eq. (1)], it is desirable that inequality $p_0 > p_S$ be met with some reserve. In this case the electron in the T-space from the start at $x=0$ (see Fig. 3) is moving with maximal

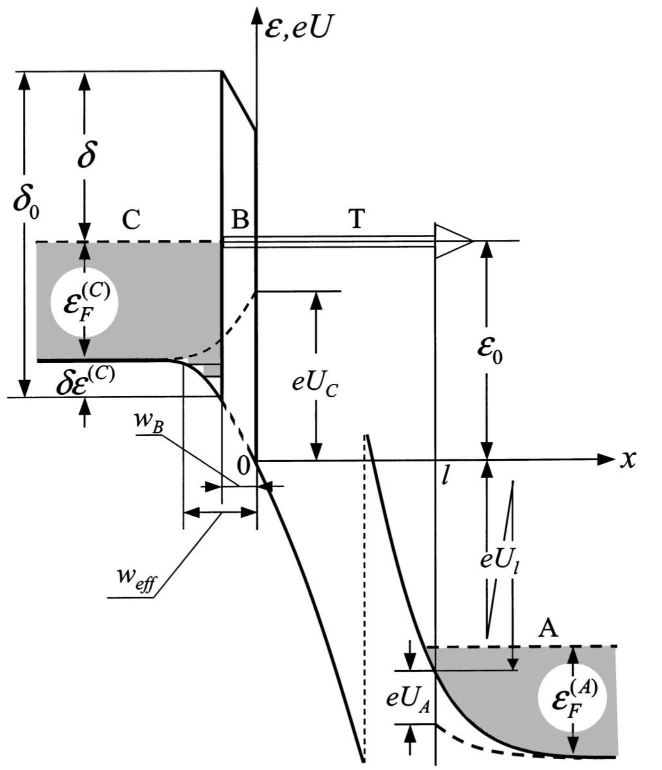

FIG. 3. Qualitative sketch of nonequilibrium potential distribution for the considered working regime. U_l is a voltage drop across T space. U_C is a voltage drop across an emitter region: an accumulation layer plus the tunnel barrier. U_A is a voltage drop across a depletion layer in n^+-anode.

(saturated) velocity V_S, and Eq. (1) can be approximately reduced to

$$\varepsilon(p) \cong V_S(p - p_S). \tag{2}$$

The value of $V_S p_S$, which can serve as an approximate measure for the necessary values of $\varepsilon_0 = \varepsilon(p_0)$, is estimated as $\sim$0.25 eV for $In_{0.53}Ga_{0.47}As$, $\sim$0.16 eV for InAs, and $\sim$0.075 eV for InSb. Below we have in mind just these three semiconductors as the probable materials for the T-space (as well as for the n^+-cathode and the n^+-anode) since in each of them the L-valley bottoms are at the level of $\varepsilon_L \sim 0.7$ eV that is much higher. To form the tunnel barrier, we need to use a wider-band-gap material. The alloy $(In_{0.53}Ga_{0.47}As)_{1-x}(In_{0.52}Al_{0.48}As)_x$ could serve as an isomorphic partner for $In_{0.53}Ga_{0.47}As$, and $(InAs)_{1-x}(InP_{0.69}Sb_{0.31})_x$ could be an isomorphic partner of InAs. Since the tunnel barriers are very thin, pseudomorphic structures can also be employed.

II. POTENTIAL STRUCTURE

In this section, we consider more thoroughly a potential structure in the T-space. Since the T-space, the n^+-cathode and the n^+-anode are grown from the same materials and the latter two are heavily doped, the Fermi level in the equilibrium state is placed high in the conduction band not only in the n^+-cathode and the n^+-anode but in the very short undoped T-space (Fig. 1). Such an inhomogeneous picture takes place both in the absence [Fig. 1(a)] and in the presence [Fig. 1(b)] of the tunnel barrier between the T-space and the n^+-cathode. We have an inhomogeneous electron enhancement of T-space and some weak depletion in the boundary-adjacent layers of the n^+-regions. An external voltage applied to the structure, which is depicted in Fig. 1(b), leads to an electron current flowing from the n^+-cathode to the n^+-anode. This substantially changes the pictures of the potential and electron concentration distributions between the n^+-regions. All the qualitative stages of evolution of these potential distributions are shown in Fig. 2. We can see that as a result of an increase in the applied voltage, not only the electric field in the T-space changes noticeably but also a potential distribution in and around the tunnel barrier significantly varies. As a result of these changes, a virtual (effective) cathode, which is initially placed (for very small currents) in the T-space (potential curves 1, 2, 3 in Fig. 2), leaves this region. The depletion layer initially placed in the n^+-cathode near the tunnel barrier transforms into an accumulation layer. An effective tunnel barrier rising over the Fermi level position in the n^+-cathode becomes lower and lower, and its form also changes. As a result of these potential variations, the tunnel current increases. The main part of this tunnel current is concentrated close to the Fermi level, as has been pointed out above. Simultaneously, while lowering the effective tunnel barrier, the energy of electrons emitting from this barrier to the T-space increases. This energy is designated as $\varepsilon_0^{(4)}$, $\varepsilon_0^{(5)}$, and $\varepsilon_0^{(6)}$ for potential curves 4, 5, and 6 in Fig. 2. It includes the Fermi energy in the n^+-cathode, $\varepsilon_F = \varepsilon_F^{(C)}$, to which we need to add an energy depth of the accumulation layer in the n^+-cathode, $\delta\varepsilon^{(C)}$, and a voltage drop in the tunnel barrier (in the energy units)

$$\varepsilon_0 \cong \varepsilon_F^{(C)} + \delta\varepsilon^{(C)} + eE_B w_B, \tag{3}$$

where E_B is an electrical field in the barrier, which becomes almost homogeneous, and w_B is the barrier thickness.

As it was indicated above, T-space electrons need to be emitted with sufficiently large values of energy ε_0 exceeding $\sim V_S p_S$. Such energies allow us to use the linear dispersion relation Eq. (2) instead of Eq. (1). We do not calculate here a depth $\delta\varepsilon^{(C)}$ of the accumulation layer, which increases with an increase in the voltage. Such a calculation is the subject of the special problem, taking into account the size quantization of an electron gas in this layer.

We are interested in such voltages across the diode when a potential distribution corresponds to potential curves 5 and 6 in Fig. 2. An example of such a distribution is presented separately in Fig. 3. An electric field in the tunnel barrier and a depth of the accumulation pocket $\delta\varepsilon^{(C)}$ are completely determined by the value of the electric field, $E(0)$, in the T-space at its boundary with the tunnel barrier ($x=0$). Therefore, the height of the effective barrier over the Fermi level $\delta = \delta_0 - \delta\varepsilon^{(C)} - \varepsilon_F^{(C)}$ is also determined by the field $E(0)$ such as the electric field in the barrier: $E_B = E(0)\kappa_D^{(T)}/\kappa_D^{(B)}$, where $\kappa_D^{(T)}$ and $\kappa_D^{(B)}$ are static dielectric constants in the T-space and the tunnel barrier, respectively. As a result, a tunnel current emitted from the n^+-cathode to the T-space in the form of a beam with the energy $\varepsilon = \varepsilon_0[E(0)]$ is determined completely by the field $E(0)$

$$j = j_T[E(0)]. \tag{4}$$

III. STATIC *JV*-CHARACTERISTIC

A static JV-characteristic is determined by the following equations:

$$j = eV(p)n, \tag{5}$$

$$V(p)dp/dx = eE, \tag{6}$$

$$\kappa_D dE/dx = en = j/V(p), \tag{7}$$

where $p = p_x$ is an electron momentum in the beam, $V(p) = d\varepsilon(p)/dp$ is electron velocity, $\varepsilon(p)$ is a kinetic energy, n is an electron concentration, and $\kappa_D = \kappa_D^{(T)}$. As a result of integrating Eqs. (5)–(7), we can obtain the required JV-characteristic in the following form:

$$(2ej/\kappa_D)^{1/2} l = \int_{p_0}^{p_l} V(p)dp/[p - p_0 + p^{(0)}(j)]^{1/2}, \tag{8}$$

where p_0 is determined by the energy of the entering T-space electron (see Fig. 3)

$$\varepsilon_0 = \varepsilon(p_0), \tag{9}$$

p_l is determined by the analogous equation

$$\varepsilon_0 + eU_l = \varepsilon(p_l), \tag{10}$$

U_l is the voltage drop across the T-space (see Fig. 3), and $p^{(0)}(j)$ is determined by the formula

$$p^{(0)}(j) = e\kappa_D \mathrm{E}^2(j)/2j, \tag{11}$$

in which $\mathrm{E}(j) = E(0)$ for a certain value of j. [Note that $E(0) = \mathrm{E}(j)$ is the converted Eq. (4).]

In the general case for the dispersion relation Eq. (1) the required JV-characteristic can be obtained numerically.[8] But the calculation is substantially simplified if the linear dispersion relation Eq. (2) is valid for the total electron beam across the whole T-space. Then

$$U_l = \mathrm{E}(j)l + jl^2/2\kappa_D V_S. \tag{12}$$

The first component on the right side of Eq. (12) corresponds to the homogeneous electric field $\mathrm{E}(j) = E(0)$ in all the T-space, and the second component takes into account the space charge effect: a linear increase in $E(x)$ from the cathode to the anode. Note that neither p_0 nor $\varepsilon_0 = \varepsilon(p_0)$ participates in Eq. (12). They take part only in its criteria of validity.

IV. ALTERNATING CURRENT WITH FREQUENCY ω

The equations defining a small alternating current with angular frequency ω have the following form (see Ref. 8):

$$j' = eVn' + enm^{-1}(p)p', \tag{13}$$

$$\kappa_D(\omega)dE'/dx = en', \tag{14}$$

$$dj'/dx + ie\omega n' = 0, \tag{15}$$

$$i\omega p' + Vdp'/dx + m^{-1}(p)p'dp/dx = eE', \tag{16}$$

where the primed values j', n', p', and E' are complex functions of x. To obtain alternating electron current density, electron concentration, electron momentum, and electric field, we should multiply j', n', p', and E', respectively, by $\exp(j\omega t)$. Since

$$j'(x) + i\omega\kappa_D(\omega)E'(x) = J', \tag{17}$$

where a total current density $J' \exp(i\omega t)$ is independent of x, we can obtain from Eqs. (13)–(17)

$$\left(V\frac{d}{dx} + i\omega\right)\left(V\frac{d}{dx} + i\omega + m^{-1}(p)\frac{dp}{dx}\right)p' + \frac{e^2 n}{\kappa_D(\omega)} m^{-1}(p)p' = \frac{eJ'}{\kappa_D(\omega)}, \tag{18}$$

where $m^{-1}(p) = d^2\varepsilon(p)/dp^2$. In the general case of the nonparabolic dispersion relation (1), Eq. (18) can be solved only numerically.[8] But in the specific case of the linearized relation (2), Eq. (18) is substantially simplified since $m^{-1}(p) = 0$ and we have

$$(V_S d/dx + i\omega)^2 p' = eJ'/\kappa_D(\omega). \tag{19}$$

Because of this simplification, we can obtain numerous results in analytic form.

Equation (19) as well as Eq. (18) should be solved with boundary conditions

$$j'(0) = \sigma_S E'(0), \tag{20}$$

where $\sigma_S = \sigma_S[E(0)]$ is a differential tunnel transparence of the tunnel barrier B, and

$$\varepsilon_0' \equiv V_S p'(0) = eE'(0)w_{\mathrm{eff}}. \tag{21}$$

The meaning of Eq. (21) can be clarified from Fig. 4. Variations of the field $E(0)$ lead to variations of the energy ε_0 because this field determines both an electric field E_B in the tunnel barrier and a depth of the accumulation layer $\delta\varepsilon^{(C)}$ [see Eq. (3)]. We should use in boundary conditions (20) and (21) $E'(0) = (1/e)(V_S d/dx + i\omega)p'|_{x=0}$.

In a quasistatic tunnel barrier version, the above-introduced new parameters $\sigma_S = \sigma_S[E(0)]$ and w_{eff} can be calculated as a result of some treatment of the stationary equations. For example, σ_S can be found as a result of a simple differentiation of Eq. (4)

$$\sigma_S = dj_T/dE(0). \tag{22}$$

But such an approach can be unrealistic for sufficiently high frequencies. The validity of Eq. (22) can be directly connected to the tunneling itself, which is not instantaneous. There exists a finite time of tunneling τ_S (see Ref. 10 as a review) associated with the passage of an electron under a tunneling barrier. The quasistatic approach anticipates $\omega\tau_S \ll 1$. For a triangular barrier, the time τ_S can be estimated by the following formula:[11,12]

$$\tau_S = (2m_B\delta)^{1/2}/eE(0), \tag{23}$$

where δ is the height of the triangular barrier for the level of the tunnel percolation (that is for $\varepsilon = \varepsilon_F^{(C)}$), and m_B is an electron effective mass in the barrier. If $m_B = 0.042m_0$ is selected where m_0 is the free electron mass $\delta = 0.2$ eV and

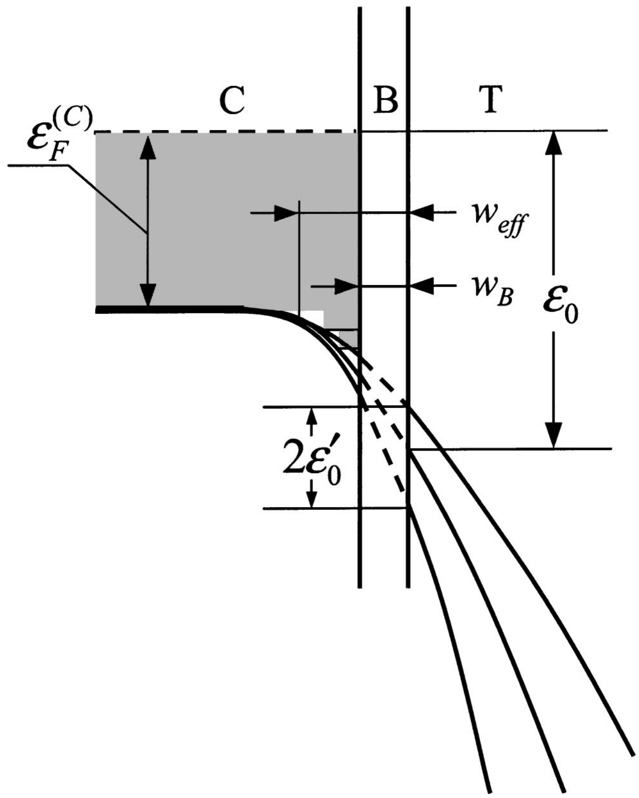

FIG. 4. Variations of energy ε_0 as a result of an alternating electric field $E'(0)$ effect.

$E(0)=10^5$ V/cm, then $\tau_S \cong 0.3\times 10^{-13}$ s. This means that the inequality $\omega\tau_S \ll 1$ is not satisfied for $f=8$ THz (or $\omega=2\pi f\sim 50$ THz), but for $f\leqslant 1$ THz a quasistatic approach is realistic. For a rectangular barrier with a thickness w_B, a quasiclassic approximation leads to an estimate

$$\tau_S = m_B^{1/2} w_B/(2\delta)^{1/2}, \tag{24}$$

that is a time τ_S can be decreased by simultaneously thinning and heightening the barrier.

Instead of the boundary condition (20), we can use an equivalent condition

$$J' = [\sigma_S(\omega)+i\omega\kappa_D(\omega)]E'(0). \tag{25}$$

Solving Eq. (19) with the boundary conditions (21) and (25), we obtain

$$p'(x)=\frac{eJ'}{\omega^2\kappa_D(\omega)}\left[-1+\left(1+\frac{\omega[\omega\kappa_D(\omega)w_{\mathrm{eff}}+i\sigma_S x]}{V_S[\sigma_S+i\omega\kappa_D(\omega)]}\right)\times\exp(-i\omega x/V_S)\right], \tag{26}$$

$$E'(x)=\frac{iJ'}{\omega\kappa_D(\omega)}\left[-1+\frac{\sigma_S}{\sigma_S+i\omega\kappa_D(\omega)}\exp(-i\omega x/V_S)\right]. \tag{27}$$

By integrating $E'(x)$ from $x=0$ to $x=l$, we calculate an alternating voltage, U_l', across the T-space and its impedance

$$Z=U_l'/J'=R+iX \tag{28a}$$

with

$$R=\frac{l^2}{\kappa_D(\omega)V_S}\left[\frac{\vartheta}{\theta^2}\times\frac{\vartheta(1-\cos\theta)+\theta\sin\theta}{\vartheta^2+\theta^2}\right], \tag{28b}$$

$$X=\frac{l^2}{\kappa_D(\omega)V_S}\left[-\frac{1}{\theta}+\frac{\vartheta}{\theta^2}\,\frac{\vartheta\sin\theta-\theta(1-\cos\theta)}{\vartheta^2+\theta^2}\right] \tag{28c}$$

where $\theta=\omega l/V_S$, $\vartheta=\sigma_S(\omega)l/V_S\kappa_D(\omega)$.

If $\vartheta\ll\theta$, resistance R and, consequently, conductance $G=R/(X^2+R^2)$ are negative in the almost complete intervals where $\sin\theta<0$ (that is at $\pi<\theta<2\pi$, $3\pi<\theta<4\pi$, and so on). But because of the inequality $\vartheta/\theta\ll 1$, values of the resistance (or the conductance) are very small in comparison with the total impedance [or the total admittance $Y=G+iB=(R-iX)/(R^2+X^2)$]. Therefore, it is necessary to narrow the θ-windows, in which R is negative, and increase the values of ϑ. In the first of the above-mentioned θ-windows, the optimal value of θ should be near $\theta=3\pi/2$ where $\sin\theta=-1$. Selecting this value of θ, we look for such a value of ϑ, for which absolute value of the so-called quality factor[3] (QF) $\mathrm{QF}=B/G=-X/R$ is minimal. (In accordance to Ref. 3, the desirable QF for transit time oscillators should be negative and not very large on the absolute value). In our case, the approximate formula for QF is

$$\mathrm{QF}\cong\theta(\vartheta^2+\theta^2)/\vartheta[\vartheta(1-\cos\theta)+\theta\sin\theta].$$

For $\theta=3\pi/2$, we have $\mathrm{QF}\cong(3\pi/2)(1+\xi^2)/\xi(1-\xi)$ where $\xi=2\vartheta/3\pi$, and the optimal value of QF is reached at $\xi=\sqrt{2}-1$ and equal to $-3\pi/(\sqrt{2}-1)\cong-22.75$. A more accurate calculation can decrease the absolute value of this optimal QF not very substantially. We see that parameters of the optimal design for the selected frequency ω should be

$$V_S/l\cong 2\omega/3\pi=4f/3, \tag{29a}$$

$$\sigma_S(\omega)/\omega\kappa_D(\omega)=\sqrt{2}-1. \tag{29b}$$

Equation (29a) is a standard transit time condition and relates only to the length and material of the T space. Equation (29b) is mainly a requirement to the tunnel barrier, which should be optimal for the selected frequency and be matched to both the T-space and the n^+-cathode. An increase in the oscillatory frequency requires not only shortening the T-space length with a desirable increase in V_S but also simultaneously increasing the differential transparence of the tunnel barrier $\sigma_S(\omega)$ in the vicinity of the Fermi energy in the n^+-cathode.

Note that the obtained comparatively large absolute value of QF ($\sim$20) is not connected specifically with the transport ballisticity or with very high oscillatory frequencies. The optimal correlation between ϑ and θ, and the optimal value of QF are invariants of the theory, and they are connected only with the assumed saturation of the electron transport velocity in T-space. The ballisticity is necessary only to legalize such high values of V_S as $(1-2)\times 10^8$ cm/s.

The maximum values of the T-space length $l_{\max}$ and the minimum oscillatory frequencies, which can be still related to the ballistic regime in T-space, are determined by the time of electron scattering out of the beam. In accordance with numerous calculations of scattering times with absorption and emission of polar optical phonons (LO scattering) in the Γ-valley, τ_{LO}, the latter saturates with an increase in energy in the same energy interval where electron velocity saturates. This saturated time typically exceeds[13–15] 10^{-13} s, and we obtain the estimation: $l_{\max}=V_S\tau_{\mathrm{LO}}\cong 10^{-5}$ cm. The actually measured[16] free path length of hot electrons in a very pure InGaAs crystal is $\sim 1.5\times 10^{-5}$ cm for $T=2$ K. The values of τ_{LO} in GaAs measured and also collected in Refs. 17 and 18 for electron energies 0.1–0.4 eV are in the range $(1-2)\times 10^{-13}$ s.

V. DIFFUSIVE ELECTRON TRANSPORT IN T-SPACE

Our presentation in the previous sections has been based on the hypothesis of ballistic electron transport between the n^+-cathode and the n^+-anode. The saturation of a ballistic velocity for the nonparabolic dispersion relation (1) allows us to obtain simple analytic results. Now we consider such a modification of our model when we keep an assumption of the saturated transport velocity for electrons in an electric field but reject an assumption of the ballisticity in T-space. Instead of a ballistic transport, we assume a diffusive electron transport with numerous collisions in the T-space. To deduce a static JV-characteristic, we should reject Eq. (6) completely and rewrite Eq. (5) in the form

$$j=ev_D(E)n, \tag{30}$$

where $v_D(E)$ is drift electron velocity, which has replaced velocity $V(p)$. We need also to produce the same replacement in Eq. (7). Note that we neglect all of the possible gradient components in Eq. (30) (such as a diffusion, thermodiffusion, etc.). This means that we assume absence of any sharp gradients in T-space. For an electric field in the T-space with taking into account Eqs. (7) and (30), we obtain

$$\kappa_D v_D(E)\,dE/dx=j. \tag{31}$$

If a drift velocity $v_D(E)$ is saturated [$v_D(E)=v_S=$const], a solution of Eq. (31) with the boundary condition (4) leads to

$$E(x)=\mathrm{E}(j)+jx/\kappa_D v_S \tag{32}$$

from where immediately a JV-characteristic in the form Eq. (12) follows with the replacement of saturated ballistic velocity V_S by saturated drift velocity v_S.

In the nonstationary case for a small harmonic signal with a frequency ω and for the same saturated drift velocity $v_D(E)=v_S$, we should replace Eq. (13) by the analogous equation

$$j'=ev_S n', \tag{33}$$

protecting Eqs. (14) and (15) in the invariable form, and rejecting completely Eq. (16). Naturally, the reduced system of equations does not require the boundary condition (21): only Eq. (20) is sufficient. [Recollect that Eq. (21) has been unclaimed even in the ballistic case: for example, in solutions (26) and (27) and in Eqs. (28a), (28b), and (28c)]. We can find from Eqs. (15) and (33) by taking into account Eq. (20)

$$j'(x)=\{J'\sigma_S(\omega)/[\sigma_S(\omega)+i\omega\kappa_D(\omega)]\}\exp(-ix\omega/v_S). \tag{34}$$

An electric field $E'(x)$ is presented by Eq. (27) after replacing V_S with v_S. We need to produce the same replacement in Eqs. (28b) and (28c) to obtain components R and X.

As we see, the ballistic and diffusive cases coincide with each other in the form of the final results: the same equations and formulas, the similar invariants and optimal correlations (for example, the optimal value of QF). But these cases operate not only with different velocities V_S and v_S, but, as a result, with different values of ω, $\sigma_S(\omega)$, and l.

VI. WEAK NONBALLISTICITY

In the previous section, we assumed that a tunneling electron beam transforms immediately after leaving the tunnel barrier B into another electron subsystem with drift velocity v_S, which is much smaller than V_S. Such an assumption is not evident since this drift velocity is formed as a result of numerous scatterings including intervalley transfers. Below we present a certain simplified model, which allows us to model an inertial and nonlocal ballistic-diffusive transfer. We introduce a finite time τ for a transfer from the ballistic beam with a saturated velocity V_S to a diffusive current with a saturated drift velocity v_S. Such a situation can be realized if the considered ballistic-diffusive transfer occurs across an intervalley ΓL-scattering.

Assume that the tunnel barrier emits ballistic electrons and their current density j_1 in a stationary electric field decreases in accordance with the following equation:

$$dj_1/dx=-en_1/\tau, \tag{35}$$

where τ is the above-mentioned time of the ballistic-diffusive transfer, and n_1 is the ballistic electron concentration

$$j_1=eV_S n_1. \tag{36}$$

The ballistic-diffusive transfer leads to the increasing second current with current density

$$dj_2/dx=en_1/\tau \tag{37}$$

with

$$j_2=ev_S n_2. \tag{38}$$

Note that we assume an absence of the back diffusive-ballistic transfer. Adding to Eqs. (35)–(38) the Poisson equation

$$\kappa_D dE/dx=e(n_1+n_2) \tag{39}$$

and using Eq. (4) and the condition $j_2(0)=0$ as the boundary conditions, we can obtain a static JV-characteristic in the following form:

$$U_l=\mathrm{E}(j)l+(j/\kappa_D v_S)\{l^2/2+(V_S-v_S)l\tau + V_S(V_S-v_S)\tau^2[1-\exp(-l/V_S\tau)]\}. \tag{40}$$

Equation (40) transforms into Eq. (12) if $\tau=\infty$. If $\tau=0$, Eq. (40) transforms into the same Eq. (12) but with the replacement of V_S by v_S. The result of such replacement can be very substantial if $V_S \gg v_S$. In particular, the leading role on the right side of Eq. (12) can transfer from the first component (tunneling) to the second one (space charge). For example, consider the specific case when

$$V_S \tau \gg l \tag{41}$$

and only a small part of ballistic electrons is able to transfer into the diffusive subsystem during their travel across T-space. Nevertheless, we obtain

$$U_l = \mathrm{E}(j) l + (j l^2 / 2\kappa_D V_S)(1 + l/3 v_S \tau) \tag{42}$$

and Eq. (42) is somewhat different from Eq. (12) if the strong inequality $3 v_S \tau \gg l$ takes place together with Eq. (41). But if

$$V_S \gg l/\tau \geqslant 3 v_S, \tag{43}$$

the structure of space charge in the T-space is changed: it is substantially defined by less mobile electrons with a small drift velocity.

A high-frequency admittance for a signal with a frequency ω is determined by the system of equations [which are analogous to Eqs. (13)–(15)]

$$dj_1' = e V_S n_1', \tag{44a}$$

$$dj_2' = e v_S n_2', \tag{44b}$$

$$\kappa_D(\omega) dE'/dx = e(n_1' + n_2'), \tag{45}$$

$$dj_1'/dx + i\omega e n_1' + e n_1'/\tau = 0, \tag{46a}$$

$$dj_2'/dx + i\omega e n_2' - e n_1'/\tau = 0, \tag{46b}$$

with the boundary conditions [compare with Eqs. (20) and (25)]

$$j_1'(0) = j'(0) = \sigma_S(\omega) E'(0) = J' \sigma_S(\omega) / [\sigma_S(\omega) + i\omega\kappa_D(\omega)]. \tag{47}$$

Equations (44)–(47) lead to a formula for an alternating electric field

$$E'(x) = \frac{iJ'}{\omega \kappa_D(\omega)} \left[-1 + \frac{\sigma_S}{\sigma_S + i\omega\kappa_D(\omega)} \Phi(x) \right], \tag{48}$$

where

$$\Phi(x) = \frac{i\omega\tau(1 - v_S/V_S)\exp[-(1 + i\omega\tau)x/V_S\tau] - (v_S/V_S)\exp(-i\omega x/v_S)}{i\omega\tau(1 - v_S/V_S) - v_S/V_S}.$$

We can check again that Eq. (48) transforms into Eq. (27) if $\tau=\infty$ and to the same Eq. (27) with a replacement $V_S \to v_S$ if $\tau=0$. As a result of the integration from 0 to l of both sides of Eq. (48), we obtain

$$\begin{aligned} Z &= U_l'/J' \\ &= -[i/\omega\kappa_D(\omega)] \Bigg[l + i \frac{\sigma_S[\sigma - i\omega\kappa_D(\omega)]}{\sigma_S^2 + \omega^2 \kappa_D^2(\omega)} \\ &\quad \times \frac{(v_S/V_S) + i\omega\tau(1 - v_S/V_S)}{(v_S/V_S)^2 + \omega^2\tau^2(1 - v_S/V_S)^2} \Psi(\omega) \Bigg], \end{aligned} \tag{49}$$

where

$$\begin{aligned} \Psi(\omega) &= V_S \tau (1 - v_S/V_S) \omega\tau (1 - i\omega\tau) \\ &\quad \times [1 - \exp(-\Lambda - i\Omega)]/(1 + \omega^2\tau^2) + (v_S^2/\omega V_S) \\ &\quad \times [1 - \exp(-i\Omega')], \end{aligned}$$

$\Lambda = l/V_S\tau$, $\Omega = \omega l/V_S$, and $\Omega' = \omega l/v_S$. As in the stationary case considered above, we pay our attention to the situation when a nearly ballistic electron transport with a velocity $V_S \gg v_S$ occurs and the strong inequality (41) is met. Then, for the frequencies starting with $\omega \geqslant \pi V_S/l$ the inequality

$$\omega\tau \gg 1, \quad v_S/V_S$$

is satisfied with a reserve, and Eq. (49) reduces to Eqs. (28a), (28b), and (28c). This means that a weak nonballisticity, which leads to the formation of a dense background of slow-drifting electrons and has a visible effect upon a static JV-characteristic, does not affect the considered oscillatory regime, induced by the only ballistic electron beam in T space.

VII. CONCLUSIVE REMARKS

(1) In this article, we continue to develop a theory of ballistic transit time diode oscillators. We have considered a model design for a single-transit (not cascading) unipolar T diode with a tunnel barrier electron emission. For this design, only two semiconductor materials are used: the first is for the n^+-cathode, the n^+-anode, and for the undoped T-space, and the second is for the tunnel barrier placed between n^+-cathode and the T-space. We suggest using (as a working ballistic electron energy range in the T-space) an energy interval $(\varepsilon_0, \varepsilon_L)$ where ε_0 is the starting energy of the emitted Γ-electron and ε_L is the bottom energy of the lowest noncentral valley, to which Γ-electrons can scatter effectively. The starting energy ε_0 should be selected so high that the electron could have the maximum saturated velocity $V_S \cong (1-2) \times 10^8$ cm/s while crossing the T-space. The range of this interval is ~0.5 eV for actual semiconductors.

(2) We have developed an analytic theory of static and a linear high-frequency conductivity of the above-described diode. We have shown that such a theory is distinguished practically from the analogous theory for a diffusive electron transport with a saturated drift velocity only by the values of incoming and resulting parameters. Since the drift velocity is 10–20 times less than the saturated ballistic velocity, then the diffusive transport oscillators are the same degree slower

than the ballistic oscillators for the same T-space length (and for much larger static voltage across this T-space).

(3) We have shown that for both the ballistic transport and the diffusive transport of electrons across the T-space, the considered T diodes have an identical and not very small quality factor in the most optimal regimes (~ -20). A high-frequency conductance for T diodes with a saturated electron transport velocity in the T-space is always proportional to the differential tunnel transparence of the tunnel emitter $\sigma_S(\omega)$. The noticeably lower values of a quality factor have been obtained in Refs. 8 and 9 where tunnel and over-barrier electron emissions with a zero starting energy and velocity were assumed: QF≈ -10 for the over-barrier space charge limited emission and QF≈ -3.3–3.5 for the tunnel emission. In the last case a high-frequency conductance can be nonzero even for $\sigma_S(\omega)=0$ [being connected with the components in Eq. (18), which are proportional to $m^{-1}(p)$ and eliminated from Eq. (19)].

(4) Since even a small leakage of electrons from the ballistic beam to the diffusive subsystem increases the static space charge in the T-space due to the small drift velocity of the diffusive transport, we have considered this effect on the basis of the simplest two-velocity model. The above-mentioned leakage leading to the visible decrease of a static conductance almost completely spares the high-frequency ballistic conductance in the THz range.

ACKNOWLEDGMENTS

The authors thank Dr. V. V. Mitin for friendly interest and support, Dr. J. East for useful comments, and Dr. S. Tipton for numerous notes. Z. S. Gribnikov thanks Dr. M. I. Dykman for fruitful discussions. This work was supported by the AFOSR through the MURI Program No. F 49620-00-0328 and by NSF Grant No. ECS-0099913.

[1] J. Nishizawa and Y. Watanabe, Sci. Rep. Res. Inst. Tohoku Univ. A **10**, 91 (1958).
[2] V. K. Aladinskii, Fiz. Tekh. Poluprovodn. (S.-Peterburg) **2**, 617 (1968) [Semiconductors **2**, 517 (1968)].
[3] S. M. Sze, *Physics of Semiconductor Devices* (Wiley, NY, 1981).
[4] J. Nishizawa, K. Motoya, and Y. Okuno, IEEE Trans. Microwave Theory Tech. **26**, 1029 (1978).
[5] H. Eisele and G. I. Haddad, IEEE Trans. Microwave Theory Tech. **46**, 739 (1998).
[6] P. Plotka, J. Nishizawa, T. Kurabayashi, and H. Makabe, IEEE Trans. Electron Devices **50**, 867 (2003).
[7] T. Bauer, M. Rosh, M. Claassen, and W. Harth, Electron. Lett. **30**, 1319 (1994).
[8] Z. S. Gribnikov, N. Z. Vagidov, V. V. Mitin, and G. I. Haddad, J. Appl. Phys. **93**, 5435 (2003).
[9] Z. S. Gribnikov, N. Z. Vagidov, V. V. Mitin, and G. I. Haddad, Physica E (Amsterdam) **19**, 89 (2003).
[10] R. Landauer and Th. Martin, Rev. Mod. Phys. **66**, 217 (1994).
[11] M. Büttiker and R. Landauer, Phys. Rev. Lett. **49**, 1739 (1982).
[12] B. I. Ivlev and V. I. Mel'nikov, Zh. Eksp. Teor. Fiz. **90**, 2208 (1986). [Sov. Phys. JETP **63**, 1295 (1986)].
[13] A. Ghis, E. Constant, and B. Boittiaux, J. Appl. Phys. **54**, 214 (1983).
[14] J. Bude and K. Hess, J. Appl. Phys. **72**, 3554 (1992).
[15] E. Kobayashi, Ch. Hamaguchi, T. Matsuoka, and K. Taniguchi, IEEE Trans. Electron Devices **36**, 2359 (1989).
[16] R. Teissier, D. Sicault, A. Goujon, J. l. Pelouard, F. Pardo, and F. Mollot, Appl. Phys. Lett. **75**, 103 (1999).
[17] G. Fasol, W. Hackenberg, H. P. Huges, K. Ploog, E. Bauser, and H. Kano, Phys. Rev. B **41**, 1461 (1990).
[18] C. L. Petersen and S. A. Lyon, Phys. Rev. Lett. **65**, 760 (1990).